Supporting Information

Umemura et al. 10.1073/pnas.1419272111

SI Materials and Methods

Plasmids. Dox-inducible *c-Myc* PiggyBac vectors (PB-TET-c-Myc), PB-CAG-rtTA Adv, and pCAG-PBase, were a kind gift from Drs. Hitoshi Niwa (RIKEN, Kobe, Japan), Andras Nagy (Samuel Lunenfeld Research Institute, Toronto), Austin Smith (University of Cambridge, Cambridge, UK), and Yasuhide Ohinata (RIKEN, Kobe, Japan) (1). For Dox-inducible *Kpna2* PiggyBac vectors (PB-TET-Kpna2), *Kpna2* was subcloned from pEGFP-KPNA2 (2) into the PB-TET vector. *Per2-myc* and *Cry2-myc* expression plasmids were a kind gift of Dr. Hajime Tei (Kanazawa University, Kanazawa, Japan). For *GFP-myc* expression plasmids, *EGFP* not including stop codon was subcloned from pEGFP-KPNA2 into the *Per2-myc* expression vector after removing *Per2* gene with EcoRI and XbaI.

Transfection. For Dox-inducible ESC lines (*tetO:c-myc mBmal1:luc* ESCs or $PER2^{Luc}$ ESCs and *tetO:Kpna2 mBmal1:luc* ESCs or $PER2^{Luc}$ ESCs) and *tetO:c-myc* $PER2^{Luc}$ MEFs, these cells were transfected using 10.5 μL of FuGENE 6 transfection reagent (Promega) mixed with 1 μg of pCAG-PBase, 1 μg of PB-TET-c-Myc or PB-TET-Kpna2, and 1 μg of PB-CAG-rtTA Adv. The transfected cells were cultured in a supplemented culture medium containing 1–2 μg/mL puromycin for 2–3 d. As for ESCs, the colonies were picked and cultured in an ESC medium. Subsequently, the *c-Myc* or *Kpna2* expression in these cell lines was checked by quantitative RT-PCR.

Cells stably expressing the mouse *Bmal1* promoter-driven luciferase reporter were established as described previously (3, 4). Briefly, 3 μg of mBmal1:luc-pT2A plasmid with a Zeocin selection marker and 1 μg of a Tol2 transposase expression vector (pCAGGS-TP) were diluted in 35 μL of culture medium and 12 μL of FuGENE 6 and mixed well. After a 15-min incubation period at room temperature, the mixture was added to 2–2.5 × 10^5 cells. The cells were selected using 20–100 μg/mL Zeocin (Invitrogen).

MEFs were transiently cotransfected with pEGFP-Kpna2 (5) and pcDNA3-Per2, pcDNA3-Cry2, or pcDNA3 empty vector. After 24 h, these cells were immunostained by anti-PER2 antibody or anti-CRY2 antibody as mentioned below.

Real-Time Bioluminescence Analysis. For real-time bioluminescence analysis of the cells seeded in 24-well black plates, the medium was replaced with EFM containing 0.2 mM luciferin (Promega) and 10 mM Hepes without phenol red. Before real-time monitoring, EFM containing Dox was removed by washing three times with EFM at 1-h intervals. Cells were treated with 100 nM dexamethasone (Sigma) for synchronization. The plates were set on a turntable in an in-house-fabricated real-time monitoring system developed by Dr. Takao Kondo (Nagoya University) (3). The bioluminescence from each well was counted for 1 min at 20-min intervals.

Real-Time Single-Cell Bioluminescence Imaging. For real-time bioluminescence analysis of single cells, cells were plated in 35-mm culture dishes. After cell attachment, the medium was replaced with EFM containing 10 mM Hepes, 0.2 mM luciferin, and 100 nM dexamethasone without phenol red. The dish was set on the stage of an LV-200 microscopic image analyzer (Olympus). Time-lapse images were collected at 60-min intervals with 59-min exposures.

Data Analysis. Strength of rhythmicity was defined using spectral analysis (FFT relative power) as relative spectral power density at the peak within the range of 21–26 h. For bioluminescence analysis, data were detrended by subtracting a 24-h moving average and presented as means with SD.

Immunofluorescence. Cells plated on coverslips were fixed with cold methanol for 15 min at room temperature. After washing with PBS, cells were blocked with 5% (wt/vol) skim milk for 60 min at 4 °C and then incubated with a primary antibody, anti-c-MYC 1:400 (N-262, Santa Cruz Biotechnology), anti-BMAL1 1:200 (6), anti-PER1 1:400 (AB2201, Millipore), anti-PER2 1:400 (6), anti-CRY1 1:200 (sc-5953, Santa Cruz Biotechnology), anti-CRY2 1:1,000 (CRY21-A, Alpha Diagnostic), and anti-KPNA2 1:1,000 (D168-3, MBL), overnight at 4 °C. After washing in PBS, the cells were incubated with a secondary antibody, Cy3-labeled anti-rabbit IgG antibodies 1:1,000 (Jackson), Alexa Fluor 647-labeled anti-goat IgG antibodies 1:1,000 (Jackson), Alexa Fluor 647-labeled anti-rat IgG antibodies 1:1,000 (Jackson), or Cy3-labeled anti-guinea pig IgG antibodies 1:1,000 (Jackson), and nuclei were stained with Hoechst 33342 (Nacalai Tesque) for 10 min at room temperature. The cells were washed in PBS and mounted with PermaFluor Mountant Medium (Thermo Electron Corporation). The cells were observed using an LSM510 confocal laser scanning microscope (Zeiss).

Quantitative RT-PCR. Cultured cells were washed three times using ice-cold PBS. Cells were harvested in 500 μL of Isogen reagent (Nippon Gene), and total RNA was extracted. As for ESCs, feeder cells were removed and ESCs were harvested. A Power SYBR Green PCR Master Mix (Applied Biosystems) was used. Transcription levels were determined in triplicate and normalized to the level of 18S ribosomal RNA. Primer sequences are shown in Table S1. Quantitative RT-PCR analysis was performed using a StepOnePlus real-time PCR system (Applied Biosystems). The amplification protocol comprised an initial incubation at 95 °C for 2 min and 40 cycles of 95 °C for 30 s and 60 °C for 30 s, followed by dissociation-curve analysis to confirm specificity.

GST Pull-Down Assay. Expression and purification of GST-KPNA2 were performed as described previously (2). COS-7 cells were transfected with plasmids using Lipofectamine 3000 (Invitrogen). At 48 h after transfection, cells were lysed in 0.3 mL hypotonic buffer [0.2% (vol/vol) Nonidet P-40, 5 mM Hepes (pH 7.3), 10 mM potassium acetate, 2 mM magnesium acetate, 2 mM DTT, 1 mM PMSF, and 1 μg/mL each aprotinin, pepstatin, and leupeptin]. Lysates were sonicated and clarified by centrifugation. The supernatant was used with the addition of 20× concentrated transport buffer and incubated with GST-KPNA2 or GST beads. The beads were subsequently washed five times with transport buffer, and after the addition of sample buffer, the samples were analyzed by Western blotting with antibodies against GST or myc tags.

Whole-Transcriptome Sequencing (RNA-seq). Total RNA was extracted with an miRNeasy Mini Kit (QIAGEN), according to the manufacturer's instructions. Total RNA (0.5 μg) was depleted of ribosomal RNAs using Ribo-Zero Gold (Illumina). Sequencing libraries were constructed using a TruSeq Stranded Total RNA LT Sample Prep Kit according to the manufacturer's instruction (Illumina). Sequencing of libraries was performed on an Illumina HiScan instrument with 100-bp paired-end reads (Illumina) by the NGS Sequencing core in the Kyoto Prefectural University of Medicine. Sequence reads were mapped to the mouse genome (GRCm38/mm10) with Tophat v2.0.9 (7) using the fol-

lowing parameters: -r 90–solexa-quals–library-type fr-firststrand. To obtain reliable alignments, the reads with mapping quality less than 10 were removed by SAMtools (8). RNA abundance was quantified by Homer (9). The UCSC canonical gene set (31,469 total) was used for annotation, as previously described (6). Among UCSC known canonical genes, we assumed that a gene was expressed if there were >20 reads in the gene body. EdgeR (10) was used to determine more than twofold up- or down-regulated genes with an expression filter (>0.02 rpkm). Each half of the reads were treated separately to make genome browser views, and the browser views were normalized to display uniquely mapped reads per 50 million uniquely mapped reads with duplicates.

Microarray and Data Processing. Total RNA was isolated using RNeasy (Qiagen) and measured. mRNA expression was assayed using a Mouse Oligo chip 24k or Human Oligo chip 25k 3D-Gene (Toray Industries). Detected signals for each gene were normalized by the global normalization method (median, 25). Genes with fold change ratios greater than 2.0 in the presence or absence of Dox were determined with expression cut off (average >5).

Statistical Analysis. Statistical differences were evaluated using Student *t* tests. For multiple comparisons, one-way ANOVA followed by Bonferroni's post hoc comparisons tests were performed. All data are given as mean ± SD. All statistics were calculated using GraphPad Prism version 6.0 software.

1. Tsukiyama T, et al. (2011) Simple and efficient method for generation of induced pluripotent stem cells using piggyBac transposition of doxycycline-inducible factors and an EOS reporter system. *Genes Cells* 16(7):815–825.
2. Yasuhara N, et al. (2013) Importin alpha subtypes determine differential transcription factor localization in embryonic stem cells maintenance. *Dev Cell* 26(2):123–135.
3. Yagita K, et al. (2010) Development of the circadian oscillator during differentiation of mouse embryonic stem cells in vitro. *Proc Natl Acad Sci USA* 107(8):3846–3851.
4. Umemura Y, et al. (2013) An in vitro ES cell-based clock recapitulation assay model identifies CK2α as an endogenous clock regulator. *PLoS ONE* 8(6):e67241.
5. Yasuhara N, et al. (2007) Triggering neural differentiation of ES cells by subtype switching of importin-alpha. *Nat Cell Biol* 9(1):72–79.
6. Koike N, et al. (2012) Transcriptional architecture and chromatin landscape of the core circadian clock in mammals. *Science* 338(6105):349–354.
7. Kim D, et al. (2013) TopHat2: Accurate alignment of transcriptomes in the presence of insertions, deletions and gene fusions. *Genome Biol* 14(4):R36.
8. Li H, et al.; 1000 Genome Project Data Processing Subgroup (2009) The Sequence Alignment/Map format and SAMtools. *Bioinformatics* 25(16):2078–2079.
9. Heinz S, et al. (2010) Simple combinations of lineage-determining transcription factors prime cis-regulatory elements required for macrophage and B cell identities. *Mol Cell* 38(4):576–589.
10. Robinson MD, McCarthy DJ, Smyth GK (2010) edgeR: A Bioconductor package for differential expression analysis of digital gene expression data. *Bioinformatics* 26(1):139–140.

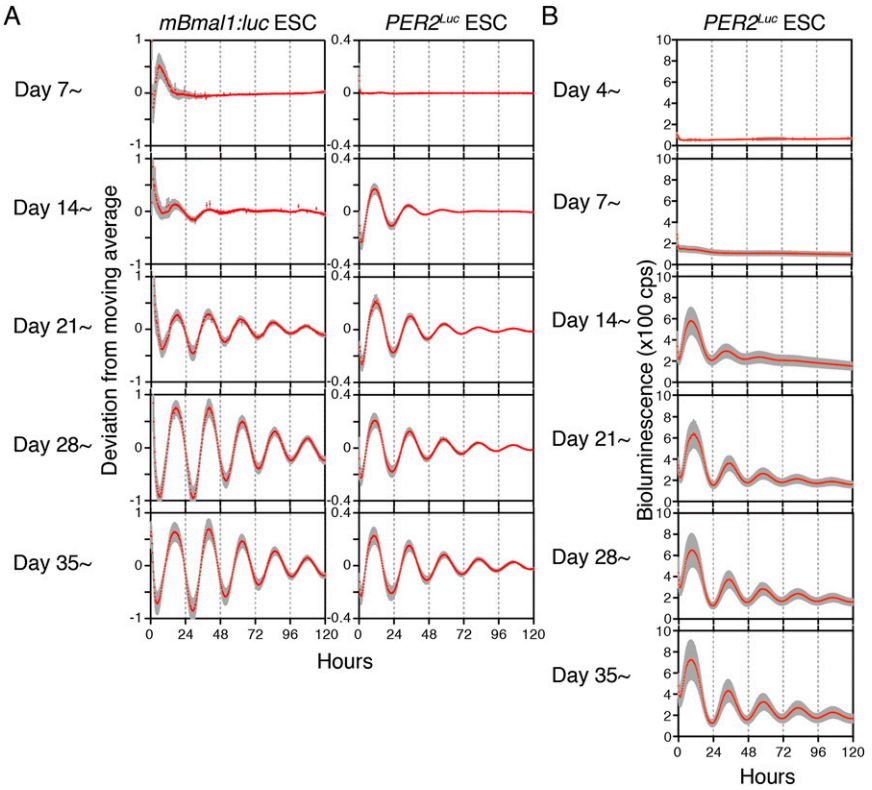

Fig. S1. Development of circadian Bioluminescence oscillation during in vitro differentiation of ESCs. (*A*) Averaged bioluminescence traces after in vitro 7-, 14-, 21-, 28-, or 35-d differentiation of ES cells (*Left*, *mBmal1:luc* ESCs; *Right*, *PER2*^{Luc} ESCs). Data, detrended by subtracting a 24-h moving average, are means with SD ($n = 24$). (*B*) Undetrended *Per2*^{Luc} driven bioluminescence rhythms during the ESC differentiation culture. Average (red line) and SD (gray) of six samples in each graph are shown.

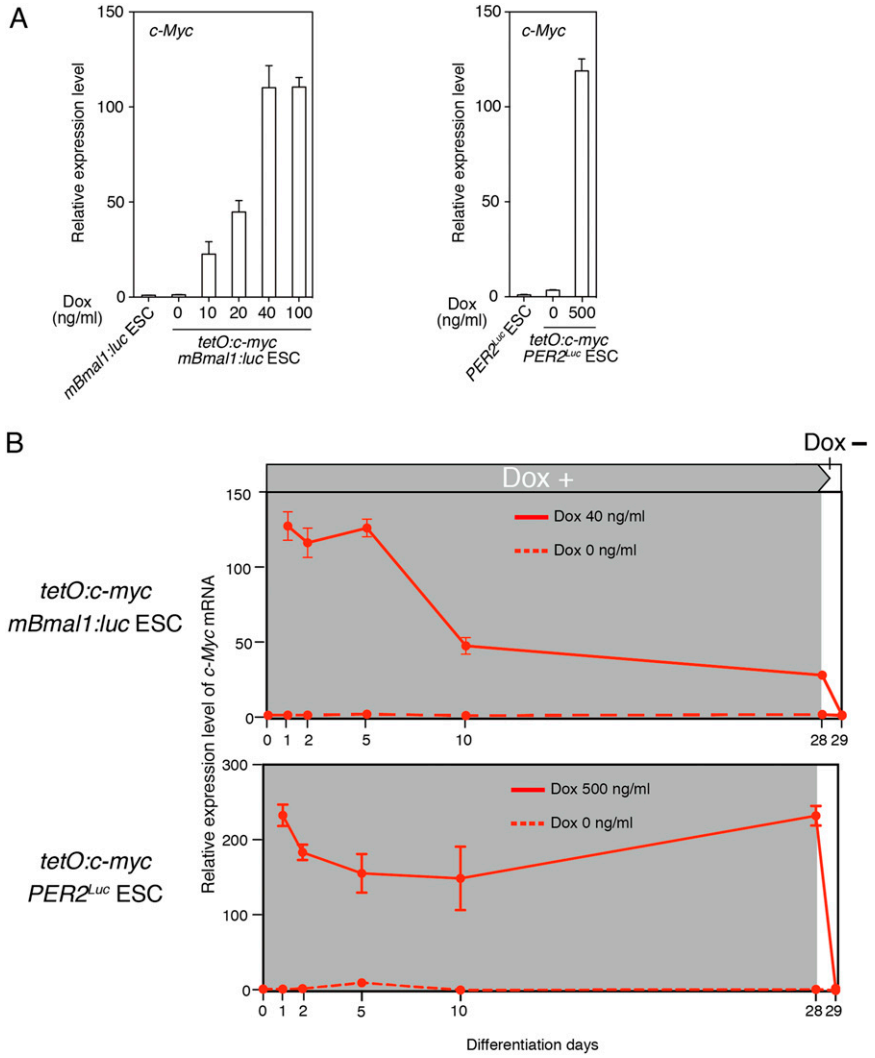

Fig. S2. Establishment of Dox-inducible *c-Myc* expression ESC lines. (*A*) Relative gene expression of *c-Myc* in *tetO:c-myc mBmal1:luc* ESCs in the absence or presence of 10, 20, 40, or 100 ng/mL Dox for 1 d (*Left*). *mBmal1:luc* ESC represents no transfected ESC. Relative expression level of *c-Myc* mRNA induced by addition of 500 ng/mL Dox in *tetO:c-myc PER2*^{Luc} ESCs (*Right*). *PER2*^{Luc} ESC represents no transfected ESC. Data shown in both panels are mean ± SD ($n = 3$). (*B*) Temporal *c-Myc* gene expression profile in the *tetO:c-myc* ESCs during the differentiation culture. Sequential relative gene expression of *c-Myc* mRNA in *tetO:c-myc mBmal1:luc* ESCs (*Upper*) and *tetO:c-myc PER2*^{Luc} ESCs (*Lower*) without (dotted red lines) and with 40 or 500 ng/mL Dox (red lines).

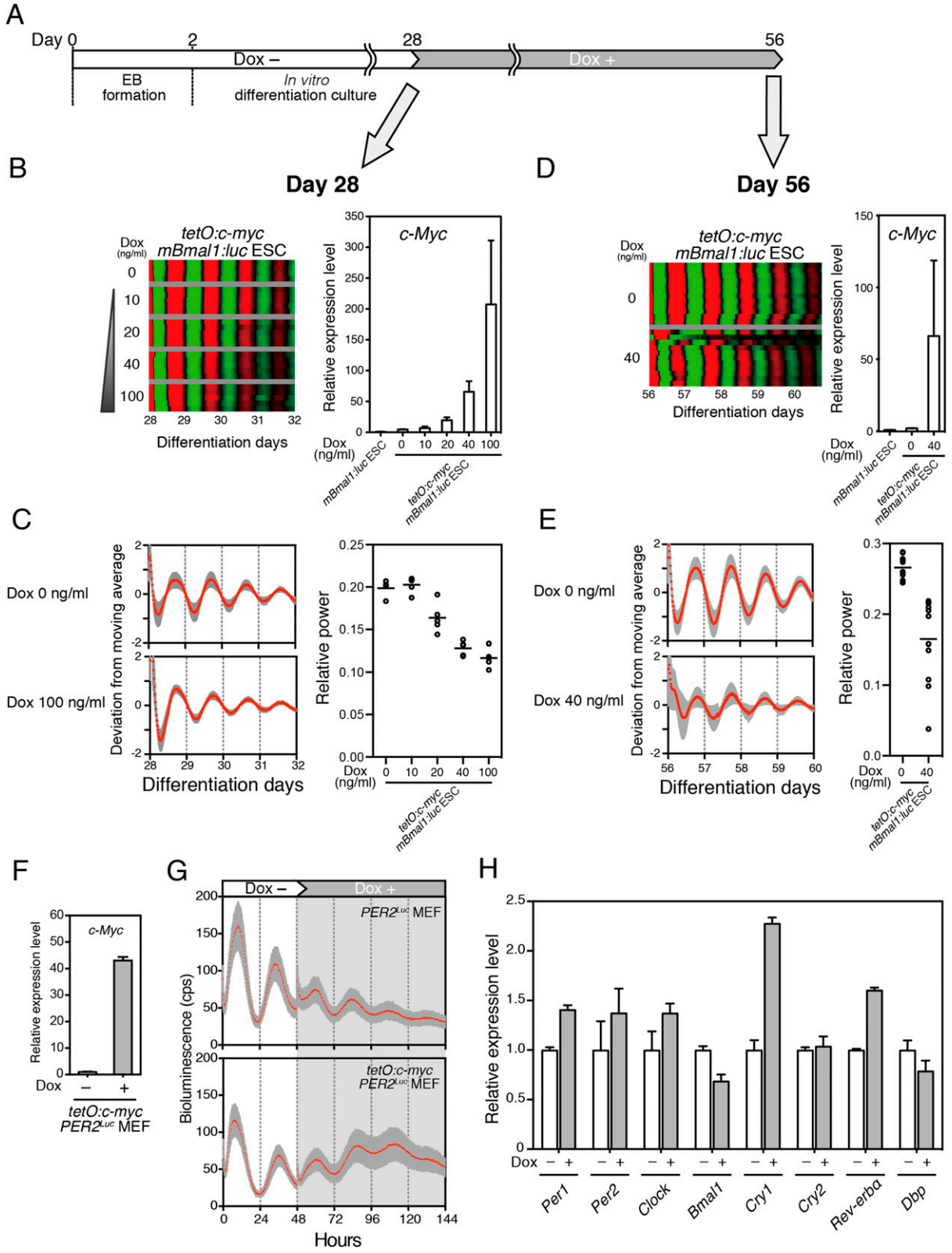

Fig. S3. Effect of *c-Myc* expression after completion of the circadian clock development. (*A*) Scheme of acute induction of *c-Myc* after in vitro 28-d-differentiated *tetO:c-myc mBmal1:luc* ESCs. In (*B*, *C*) in vitro 28-d differentiation or (*D*, *E*) in vitro 56-d differentiation, raster plots, relative expression level of *c-Myc* mRNA, averaged bioluminescence traces, and FFT spectral power analysis. After real-time monitoring in the medium containing Dox, relative expression level of *c-Myc* mRNA was examined. (*F–H*) Effect of acute overexpression of *c-Myc* in *PER2*^{Luc} MEFs. (*F*) Relative gene expression of *c-Myc* in *PER2*^{Luc} MEF cells stably expressing doxycycline-inducible *c-Myc* (*tetO:c-myc PER2*^{Luc} MEF) in the absence or presence of 10 μg/mL Dox for 1 d. Data are mean ± SD ($n = 3$). (*G*) Averaged detrended bioluminescence traces of *tetO:c-myc PER2*^{Luc} MEF cells. The light gray shading denotes the medium with 10 μg/mL Dox (red lines) or without Dox (black lines). Data, detrended by subtracting a 24-h moving average, are means with SD of eight independent samples. (*H*) Relative expression level of a set of core clock genes in the absence or presence of 10 μg/mL Dox for 1 d.

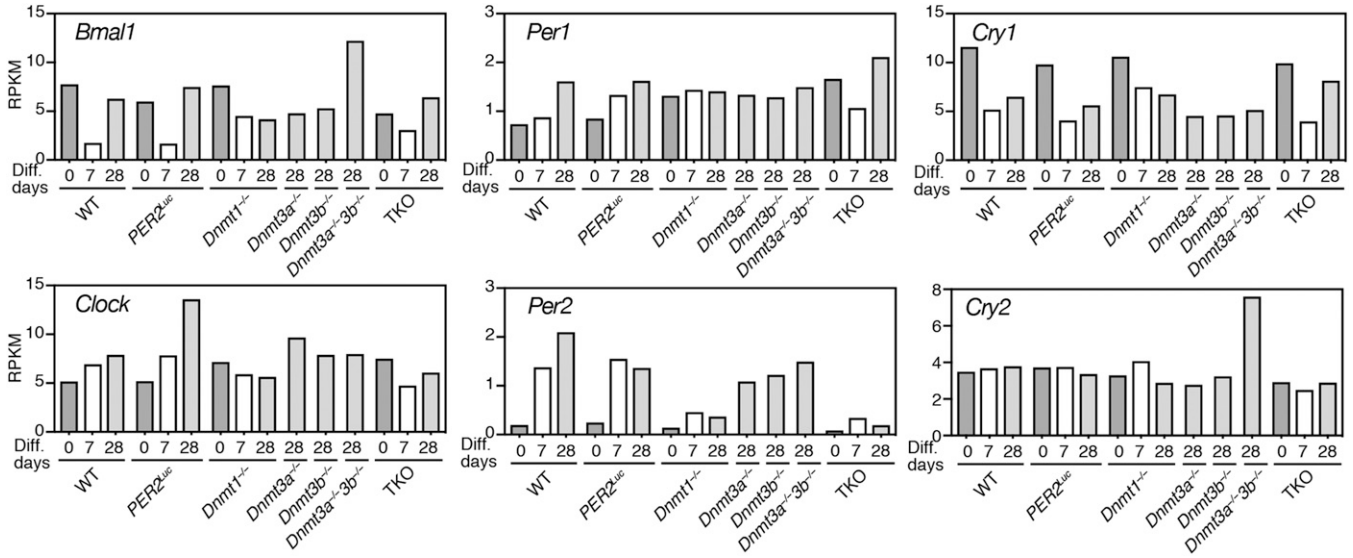

Fig. S4. Core clock genes expression profiles of in vitro 0-, 7-, or 28-d differentiation of indicated ESCs using RNA-seq. Expression profiles of core clock genes (*Bmal1, Clock, Per1, Per2, Cry1*, and *Cry2*) were analyzed in 0-, 7-, or 28-d differentiated WT and *Dnmt*-deficient ESCs.

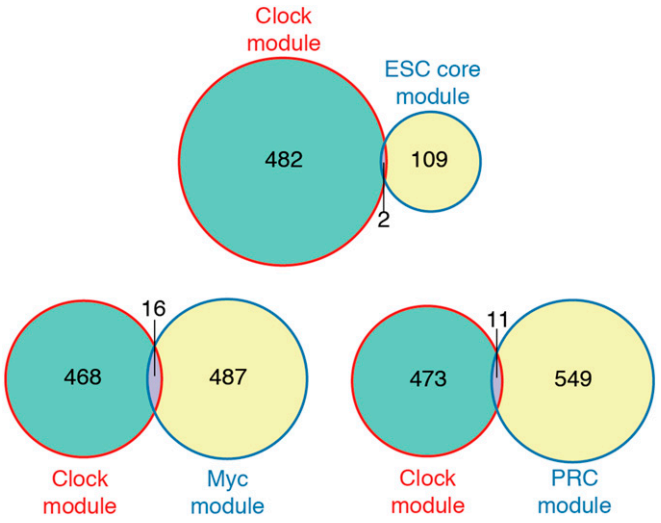

Fig. S5. Clock development correlating gene set does not overlap with ESC-core, ESC-PRC, and ESC-Myc modules. Venn diagrams comparing between the extracted gene set and ESC-related functional modules such as ESC-core, ESC-PRC, and ESC-Myc modules.

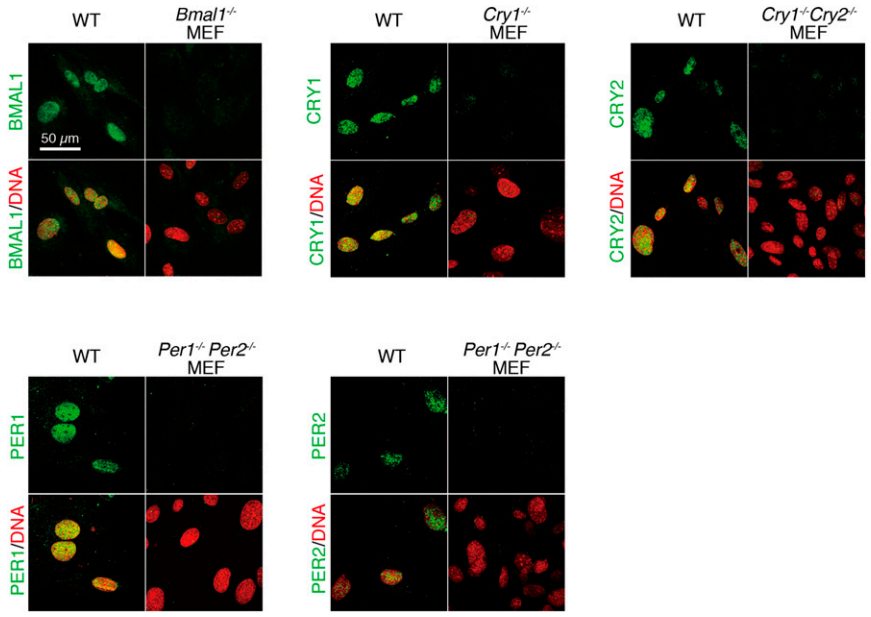

Fig. S6. Nuclear dominant expression of core clock proteins in MEFs. Immunofluorescence study using circadian clock developed MEFs against core clock proteins. In WT MEFs, BMAL1, PER1, PER2, CRY1, and CRY2 were all expressed dominantly in the nucleus, whereas knockout MEFs lacking the indicated genes lost the immunofluorescence signals against the indicated gene products. These data confirmed the specificity of antibodies for clock proteins used in this study, as well as the intact expression patterns of core clock proteins in clock-oscillating intact cells.

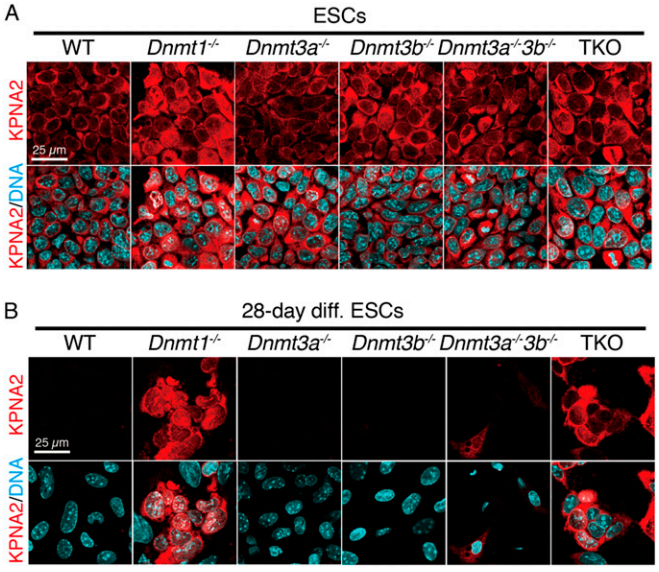

Fig. S7. Strong expression of endogenous KPNA2 (Importin-α2) protein in ESCs and 28-d-differentiated *Dnmt1*$^{-/-}$ and TKO cells. (*A*) Immunofluorescence study using anti-KPNA2 (Importin-α2) in WT and *Dnmt*-deficient ESCs. KPNA2 protein strongly expressed in all ESCs. DNA was counterstained by Hoechst 33342. (*B*) Immunofluorescence study using anti-KPNA2 (Importin-α2) in 28-d in vitro-differentiated WT and Dnmt-deficient ESCs. KPNA2 protein was highly expressed only in the *Dnmt1*$^{-/-}$ and TKO cells after the differentiation culture.

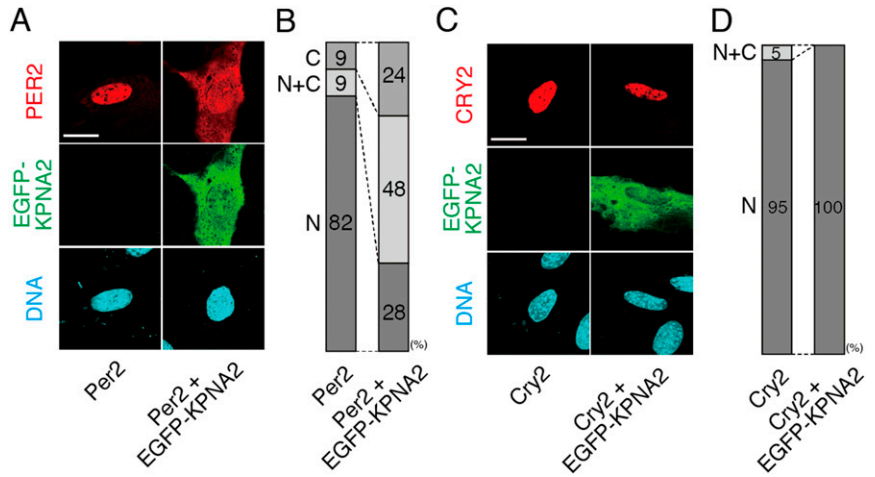

Fig. S8. Coexpression of EGFP-KPNA2 resulted in the increase of cytoplasmic PER2. (*A*) Transfection of pcDNA3-mPer2 with or without EGFP-KPNA2. Immunofluorescence using anti-PER2 was performed. (*B*) The subcellular localization of PER2 was scored as cytoplasm only "C," both cytoplasm and nucleus "N + C," or nucleus only "N." (*C*) Immunofluorescence for CRY2 with or without cotransfection of EGFP-KPNA2. (*D*) The subcellular localization of CRY2 was scored as cytoplasm only "C," both cytoplasm and nucleus "N + C," or nucleus only "N." (Scale bars, 25 μm.)

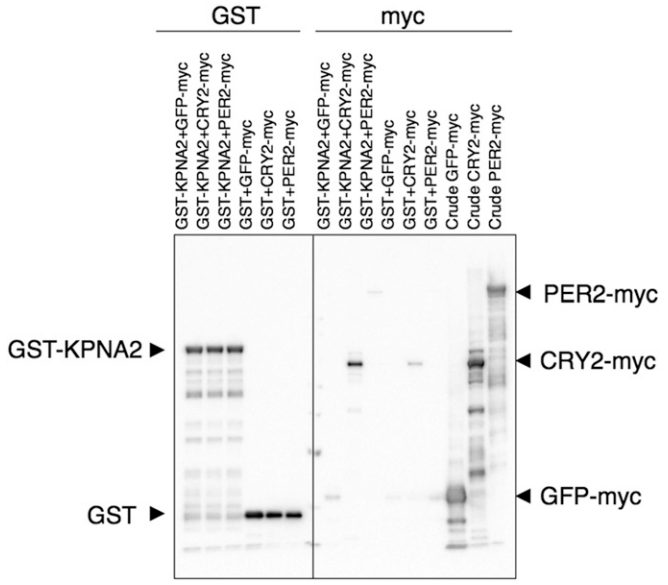

Fig. S9. GST pull-down assay examining the interaction between KPNA2 and PER2. GST pull-down assay using GST-KPNA2 and myc-tagged PER2 was performed. Immunoblotting against myc-tag showed that the signal of myc-tagged PER2 coprecipitated with GST-KPNA2 was very weak, although coprecipitated myc-tagged CRY2 signal was obvious. This indicates that the binding between KPNA2 and PER2 may be very weak.

Table S1. List of quantitative RT-PCR primers (5′ to 3′)

Gene name	Forward (F) or reverse (R) primer	Primer sequence
c-Myc	F	CCCTAGTGCTGCATGAGGAGACACC
c-Myc	R	AGGGGTTTGCCTCTTCTCCACAGAC
Oct3/4	F	CCCAATGCCGTGAAGTTGGAGAAGG
Oct3/4	R	CTGGGTGTACCCCAAGGTGATCCTC
Nanog	F	CAGATGCAAGAACTCTCCTCCA
Nanog	R	ATGGATGCTGGGATACTCCACT
Sox2	F	AAGAAAGGAGAGAAGTTTGGAGCC
Sox2	R	GAGATCTGGCGGAGAATAGTTGG
Kpna1	F	TAGAGGGAAGAGCCCACCTCCAGAA
Kpna1	R	AGCCCAGCAAGCATCAGCTAGTACA
Kpna2	F	GTTGGCACTTCTTGCAGTTCCCGAT
Kpna2	R	AATCTGCTCAACGGCGTCTAAGGGA
Kpna3	F	CAGGGGTTGTACCCTTCCTCGTACC
Kpna3	R	GAGAACCACCTGGGTCTGCTCATCA
Kpna4	F	GGCCCTGTCTTACCTTACGGATGCT
Kpna4	R	CTCGCAGTGCAGCAGTCTGAACTTT
Kpna6	F	GTCCACACGACTGACAATGACACGG
Kpna6	R	AGAGCAGTCGGGACAATACAGGCAA

Dataset S1. A list of more than twofold up- or down-regulated genes of in vitro 28-d-differentiated *tetO:c-myc* ESCs in the presence of Dox compared with in the absence of Dox, related to Fig. 2 *A* and *B*

Dataset S1

Dataset S2. The list of 2,606 overlapped genes commonly changed among the clock-disrupted conditions (all ESCs, differentiated *Dnmt1*$^{-/-}$ cells, differentiated TKO cells, and 7-d-differentiated WT and *PER2*^{Luc} ESCs) compared with the clock-oscillating cells, related to Fig. 4*A*

Dataset S2

Dataset S3. Gene lists showing commonly changed expression in the differentiated cells in the Dox^{+} of *tetO:c-myc Bmal1:luc* ESCs and *tetO:c-myc PER2*^{Luc} ESCs, related to Fig. 4*B*

Dataset S3

Dataset S4. The list of up-regulated 98 genes and down-regulated 386 genes in both clock-disrupted *Dnmt*-deficient cells and *c-Myc* over-expressed cells, related to Fig. 4*C*

Dataset S4